

# Gas-Phase Protonation of Spiropentane. A Novel Entry into the $C_5H_9^+$ Potential Energy Surface

Patrizio Cecchi,<sup>†</sup> Adriano Pizzabiocca,<sup>‡</sup> Gabriele Renzi,<sup>‡</sup> Felice Grandinetti,<sup>§</sup>  
Cinzia Sparapani,<sup>§</sup> Peter Buzek,<sup>||</sup> Paul von Ragué Schleyer,<sup>\*,||</sup> and Maurizio Speranza<sup>\*,⊥</sup>

Contribution from the Dipartimento di Agrobiologia ed Agrochimica, Università della Tuscia, Viterbo, Italy, the Dipartimento di Chimica, Università di Camerino, Camerino (MC), Italy, the Istituto di Chimica Nucleare del CNR, Area della Ricerca CNR di Roma, Rome, Italy, Institut für Organische Chemie I, Universität Erlangen-Nürnberg, Erlangen, Germany, and the Dipartimento di Studi di Chimica e Tecnologia delle Sostanze Biologicamente Attive, Università di Roma "La Sapienza", Rome, Italy

Received April 26, 1993\*

**Abstract:** The structures, stabilities, and isomerization patterns of  $C_5H_9^+$  ions arising from the gas-phase protonation of spiropentane have been investigated by nuclear-decay, radiolytic, and FT-ICR techniques combined with *ab initio* calculations. The experimental and theoretical results are consistent with the initial formation of a corner-protonated spiropentane intermediate **17**, whose lifetime in the gas phase exceeds  $7 \times 10^{-9}$  s. This local  $C_5H_9^+$  minimum is separated from the *ca.* 30 kcal mol<sup>-1</sup> more stable cyclopentyl cation as well as from dimethylallyl open-chain isomers by significant energy barriers. Persistence of **17** in the gas phase does not find any correspondence in solution. Solvation and ion-pairing effects may explain the failure to detect  $C_5H_9^+$  structures retaining the spirobicyclic framework of spiropentane in the condensed phase.

## Introduction

The exploration of the  $C_5H_9^+$  potential energy surface has not received the same level of attention as that of  $C_4H_7^+$ .<sup>1-5</sup> The generation of  $C_5H_9^+$  isomers by superacids in solution is restricted to cyclopentyl (**1**),<sup>6</sup> methylcyclobutyl (**2**),<sup>7</sup> *trans*- and *cis*-1-cyclopropylethyl (**3**, **4**),<sup>8</sup> 1,1-(**5**)<sup>9</sup> and 1,3-dimethylallyl (**6**),<sup>9,10</sup>

and 1-ethylallyl (**7**) cations.<sup>8</sup> Carbon scrambling in **1** via the pyramidal species **8** and the transition state **9** was investigated by Saunders using doubly <sup>13</sup>C labeled cyclopentyl precursors.<sup>11</sup> Evidence for the nonplanarity of the methylcyclobutyl cation (**2**) was given by Sorensen and Saunders.<sup>7</sup> Rearrangement of **2** to the cyclopropylethyl cations **3** and **4** at -25 °C could be shown to occur.<sup>8</sup> The interconversion of **3** and **4** does not follow a simple rotation along the corresponding C-C bond; instead, rearrangement via 1-ethylallyl cation (**7**) allows a lower energy pathway. Schleyer and Saunders investigated the disrotatory ring opening of different 2,3-dimethylcyclopropyl stereoisomers to generate specifically *cis*- and *trans*-1,3-dimethylallyl cations **6**.<sup>10</sup>

<sup>†</sup> University of Tuscia.

<sup>‡</sup> University of Camerino.

<sup>§</sup> Istituto di Chimica Nucleare del CNR.

<sup>||</sup> Universität Erlangen-Nürnberg.

<sup>⊥</sup> University of Rome "La Sapienza".

\* Abstract published in *Advance ACS Abstracts*, September 15, 1993.

(1) Olah, G. A.; Reddy, V. P.; Prakash, G. K. S.; *Chem. Rev.* **1992**, *92*, 69 and references therein.

(2) (a) McKee, M. L. *J. Phys. Chem.* **1986**, *90*, 4908. (b) Koch, W.; Liu, B.; DeFrees, D. J.; *J. Am. Chem. Soc.* **1988**, *110*, 7325. (c) Saunders, M.; Laidig, K. E.; Wiberg, K. B.; Schleyer, P. v. R. *J. Am. Chem. Soc.* **1988**, *110*, 7652.

(3) (a) Olah, G. A.; Kelly, D. P.; Jeuell, C. L.; Porter, R. D. *J. Am. Chem. Soc.* **1970**, *92*, 2544. (b) Staral, J. S.; Yavari, I.; Roberts, J. D.; Prakash, G. K. S.; Donovan, D. J.; Olah, G. A. *J. Am. Chem. Soc.* **1978**, *100*, 8016. (c) Staral, J. S.; Roberts, J. D. *J. Am. Chem. Soc.* **1978**, *100*, 8018. (d) Saunders, M.; Siehl, H. U. *J. Am. Chem. Soc.* **1980**, *102*, 6868. (e) Saunders, M.; Siehl, H. U. *J. Am. Chem. Soc.* **1980**, *102*, 6869. (f) Brittain, W. J.; Squillacote, M. E.; Roberts, J. D. *J. Am. Chem. Soc.* **1984**, *106*, 7280. (g) Saunders, M.; Laidig, K. E.; Wolfsberg, M. *J. Am. Chem. Soc.* **1989**, *111*, 8989. (h) Myhre, P. C.; Webb, G. G.; Yannoni, C. S. *J. Am. Chem. Soc.* **1990**, *112*, 8992. (i) Buzek, P.; Schleyer, P. v. R.; Sieber, S. *Chem. Unserer Zeit* **1992**, *26*, 116.

(4) (a) Bowen, R. D.; Williams, D. H.; Schwarz, H.; Wesdemiotis, C. *J. Chem. Soc., Chem. Commun.* **1979**, 261. (b) Cacace, F.; Speranza, M. *J. Am. Chem. Soc.* **1979**, *101*, 1589. (c) Schulte, J. C.; Houle, F. A.; Beauchamp, J. L. *J. Am. Chem. Soc.* **1984**, *106*, 7336.

(5) Kelly, D. P.; Brown, H. C. *J. Am. Chem. Soc.* **1975**, *97*, 3897 and references therein.

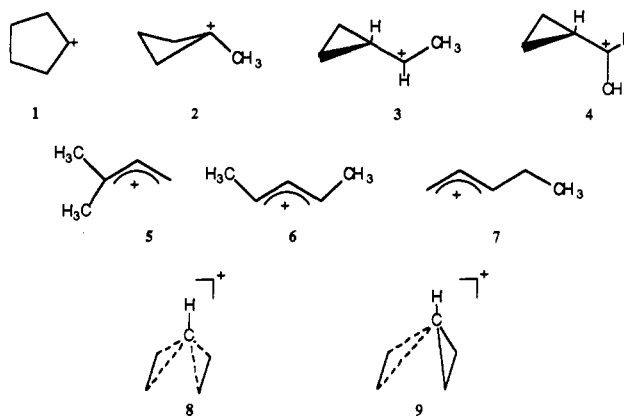
(6) (a) Schleyer, P. v. R.; Carneiro, J. W. M.; Koch, W.; Raghavachari, K. *J. Am. Chem. Soc.* **1989**, *111*, 5475. (b) Myhre, P. C.; Kruger, J. D.; Hammond, B. L.; Lok, S. M.; Yannoni, C. S.; Macho, V.; Limbach, H. H.; Vieth, H. M. *J. Am. Chem. Soc.* **1984**, *106*, 6079.

(7) (a) Saunders, M.; Krause, N. *J. Am. Chem. Soc.* **1988**, *110*, 8050. (b) Servis, K. L.; Shue, F. F. *J. Am. Chem. Soc.* **1980**, *102*, 7233. (c) Siehl, H. U. *J. Am. Chem. Soc.* **1985**, *107*, 3390. (d) Prakash, G. K. S.; Aravanaghi, M.; Olah, G. A. *J. Am. Chem. Soc.* **1985**, *107*, 6017. (e) Kirchen, R. P.; Sorensen, T. S. *J. Am. Chem. Soc.* **1977**, *99*, 6687. (f) Olah, G. A.; Jeuell, C. L.; Kelly, D. P.; Porter, R. D. *J. Am. Chem. Soc.* **1972**, *94*, 146. (g) Saunders, M.; Rosenfeld, J. *J. Am. Chem. Soc.* **1970**, *92*, 548.

(8) (a) Olah, G. A.; Spear, R. J.; Hiberty, P. C.; Hehre, W. J. *J. Am. Chem. Soc.* **1976**, *98*, 7470. (b) Falkenberg-Andersen, C.; Ranganayakulu, K.; Schmitz, L. R.; Sorensen, T. S. *J. Am. Chem. Soc.* **1984**, *106*, 178.

(9) Olah, G. A.; Spear, R. J. *J. Am. Chem. Soc.* **1981**, *103*, 4458.

(10) Schleyer, P. v. R.; Su, T. M.; Saunders, M.; Rosenfeld, J. C. *J. Am. Chem. Soc.* **1969**, *91*, 5174.


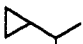
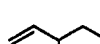
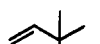





A general description of the potential energy surface of  $C_5H_9^+$  by *ab initio* methods has not yet been carried out. Only the chiral  $C_2$  structure of the cyclopentyl cation was investigated at the MP2(FULL)/6-31G\*\* level of theory.<sup>6</sup> The necessity to use electron-correlated methods and polarization functions at least on carbon (MP2/6-31G\*) was noted.<sup>12</sup> In the present study all structures have been fully optimized at the MP2(FULL)/6-31G\* level and for certain systems at MP2(FC)/6-31G\*\*.

(11) Franke, W.; Schwarz, H.; Thies, H.; Chandrasekhar, J.; Schleyer, P. v. R.; Hehre, W. J.; Saunders, M.; Walker, G. *Chem. Ber.* **1981**, *114*, 2808.

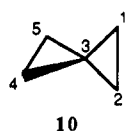
(12) (a) Carneiro, J. W. M.; Schleyer, P. v. R. *J. Am. Chem. Soc.* **1990**, *112*, 4064. (b) Buzek, P.; Schleyer, P. v. R.; Koch, W.; Carneiro, J. W. M.; Vancik, H.; Sunko, D. E. *J. Chem. Soc., Chem. Commun.* **1991**, 671. Sieber, S.; Buzek, P.; Schleyer, P. v. R.; Koch, W.; Carneiro, J. W. M. *J. Am. Chem. Soc.* **1993**, *115*, 259.

Table I. Tritiated Product Yields from the Gas-Phase Tritonation of Spiropentane by  $^3\text{HeT}^+$  Ions

system composition (Torr) <sup>a</sup>		relative yields of products (activity, %) <sup>b</sup>							total absolute yields (activity, %) <sup>c</sup>
spiropentane	nucleophile (NuH)								
		10'	11	12	13	14	15	16	
100		100							8.1
50		100							3.6
50	<i>d</i>	100							1.1
10		100							3.4
100	12 (H <sub>2</sub> O)	37	4	4	10	3	22	20	5.5
50	12 (H <sub>2</sub> O)	31	9	4	10	2	25	19	4.5
10	11 (H <sub>2</sub> O)	29	12	4	7	2	23	22	4.0
100	9 (MeOH)	54	2	1	4	1	20	18	6.9
50	6 (MeOH)	31	7	5	9	3	24	21	5.7
10	6 (MeOH)	28	13	4	7	2	24	22	5.4

<sup>a</sup> All systems contain 4 Torr of O<sub>2</sub> and 0.6–0.9 mCi of T<sub>2</sub>. <sup>b</sup> The data represent the average of at least three independent analyses, with an uncertainty level of ca. 15%. <sup>c</sup> The absolute yields estimated from the percent ratio between the combined activity of the identified tritiated products and the activity of the  $^3\text{HeT}^+$  reagent. <sup>d</sup> 20 Torr of NMe<sub>3</sub> added.

The C<sub>5</sub>H<sub>9</sub><sup>+</sup> isomerization pattern in the gas phase, where solvation and ion-pairing effects are excluded, allows a direct comparison with the calculated potential energy surface. The protonation of the very strained<sup>13</sup> spiro[2.2]pentane (10) opens access to a great variety of possible C<sub>5</sub>H<sub>9</sub><sup>+</sup> isomers through rearrangement. The isomerization pattern was investigated under a range of experimental conditions (from 10 to 760 Torr of total pressure). Brønsted acids of different strength were used, namely,  $^3\text{HeT}^+$ , D<sub>3</sub><sup>+</sup>, C<sub>n</sub>H<sub>5</sub><sup>+</sup> (*n* = 1, 2), and *i*-C<sub>3</sub>H<sub>7</sub><sup>+</sup>, which were generated in the gas phase from their neutral precursors, *i.e.* T<sub>2</sub>, D<sub>2</sub>, CH<sub>4</sub>, and C<sub>3</sub>H<sub>8</sub>, by stationary nuclear-decay (T<sub>2</sub>)<sup>14</sup> and by radiolytic procedures (D<sub>2</sub>, CH<sub>4</sub>, and C<sub>3</sub>H<sub>8</sub>).<sup>15</sup> The rearranged carbocations were identified by trapping with different nucleophiles (NuH), like H<sub>2</sub>O and MeOH.



## Results

Two different methods, nuclear decay and radiolysis, were used to generate the protonating agents. These Brønsted acids protonate the spiropentane and trigger the rearrangement process.

**Nuclear Decay.** Table I reports the composition of the nuclear-decay systems, the yields and identities of the tritiated products which arise from the attack of the  $^3\text{HeT}^+$  ions on gaseous spiropentane 10. The total absolute yields of products, expressed by the percent ratio of their combined activity to the activity of the nuclear-decay-generated (nucleogenic)  $^3\text{HeT}^+$ , can be calculated from the initial activity and the isotopic composition of the tritium molecules, the decay rate of tritium, the abundance of the  $^3\text{HeT}^+$  ions among the decay fragments (ca. 95%),<sup>16</sup> and the absolute counting efficiency of the detector employed.

The calculated absolute yields never exceeded 10% of the activity contained in the parent  $^3\text{HeT}^+$  ions. A larger fraction (40–50%) of the residual activity was recovered in low-boiling fragmentation products and in high-boiling oligomerization

(13) (a) Fraser, F. M.; Prosen, E. J. *J. Res. Natl. Bur. Stand.* **1955**, *54*, 143. (b) Hiller, I. J.; *Tetrahedron* **1969**, *25*, 1349. (c) Kao, J.; Radom, L. *J. Am. Chem. Soc.* **1978**, *100*, 760. (d) Gund, P.; Gund, T. M. *J. Am. Chem. Soc.* **1981**, *103*, 4458. (e) Boese, R.; Bläser, D.; Goman, K.; Brinker, U. H. *J. Am. Chem. Soc.* **1989**, *111*, 1501.

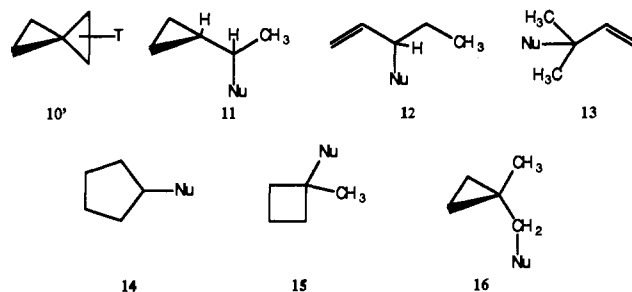
(14) (a) Cacace, F.; Speranza, M. In *Techniques for the Study of Ion-Molecule Reactions*; Farrar, J. M., Saunders, W. N., Jr., Eds.; Wiley: New York, 1988; Chapter VI. (b) Cacace, F. *Science* **1990**, *250*, 392.

(15) (a) Cacace, F. *Acc. Chem. Res.* **1988**, *21*, 215. (b) Speranza, M. *Mass Spectrom. Rev.* **1992**, *11*, 73.

(16) (a) Snell, A. M.; Pleasonton, F.; Leming, H. E. *J. Inorg. Nucl. Chem.* **1957**, *5*, 112. (b) Wexler, S. *J. Inorg. Nucl. Chem.* **1959**, *10*, 8.

derivatives. The relative proportions increase upon decreasing the partial pressure of 10. The missing activity (40–50%) is presumably carried by some intractable polymerization products or, more likely, by the formation of HT molecules, whose activity can hardly be discriminated from that contained in the starting tritium gas.

Table I shows that the tritiated spiropentane 10' is always the most abundant product (relative yield: 28–100%). When the nucleophile NuH is added to the gaseous compounds, a complex mixture of labeled Nu derivatives 11–16 (Nu: OH or OMe) results. The complexity of the tritiated product pattern demonstrates the property of the initial protonated spiropentane to follow several competing isomerization pathways.



**Radiolysis.** The absolute and relative yields of the products from the gas-phase attack of D<sub>3</sub><sup>+</sup>, CH<sub>5</sub><sup>+</sup>, C<sub>2</sub>H<sub>5</sub><sup>+</sup>, and *i*-C<sub>3</sub>H<sub>7</sub><sup>+</sup> ions on 10 in the presence of variable concentrations of added nucleophiles (NuH = H<sub>2</sub>O or MeOH) are reported in Table II, together with the composition of the irradiated mixtures. The total absolute yields of the radiolytic products are given as the percent ratio of their *G*(M) values, *i.e.* the number of molecules of product M formed per 100 eV of energy absorbed by the gaseous mixture, to the *G* values for the formation of their individual Brønsted acid precursors, namely, *G*(D<sub>3</sub><sup>+</sup>) = 3,<sup>17</sup> *G*(C<sub>n</sub>H<sub>5</sub><sup>+</sup>) = 1.9 (*n* = 1) and 0.9 (*n* = 2),<sup>18</sup> and *G*(*i*-C<sub>3</sub>H<sub>7</sub><sup>+</sup>) = 3.<sup>19</sup> These calculations, although approximate,<sup>20</sup> are an estimate of the isomerization extent undergone by the initial species from gas-phase protonation of 10.



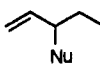
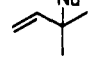
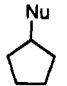
A radiolytic product pattern emerges from the results of Table II which essentially conforms to that arising from the decay

(17) Weiss, J.; Bernstein, W. *Radiat. Res.* **1957**, *6*, 603.

(18) Ausloos, P.; Lias, S. G.; Gorden, R., Jr. *J. Chem. Phys.* **1963**, *39*, 3341.

(19) (a) Ausloos, P. In *Ion-Molecule Reactions*; Franklin, J. L., Ed.; Plenum: New York, 1970. (b) Ausloos, P.; Lias, S. G. *J. Chem. Phys.* **1962**, *36*, 3163. (c) Lias, S. G.; Ausloos, P. *J. Chem. Phys.* **1962**, *37*, 877. (d) Sandoval, I. B.; Ausloos, P. *J. Chem. Phys.* **1963**, *38*, 2, 452. (e) Freeman, G. R. *Radiat. Res. Rev.* **1968**, *1*, 1.

**Table II.** Product Distribution from the Gas-Phase Protonation of Spiropentane by Radiolytically-Formed  $D_3^+$ ,  $C_nH_5^+$  ( $n = 1, 2$ ), and  $i-C_3H_7^+$  Ions

bulk gas	system composition (Torr) <sup>a</sup>		NMe <sub>3</sub>	relative yields of products (%) <sup>b</sup>				total absolute yield (%) <sup>c</sup>
		nucleophile (NuH)						
D <sub>2</sub> , 760	0.6	1.7 (H <sub>2</sub> O)	3	38	20	31	11	4
D <sub>2</sub> , 760	0.6	2.4 (H <sub>2</sub> O)	3	28	22	47	13	2
D <sub>2</sub> , 760	0.5	1.5 (H <sub>2</sub> O)		40	17	33	10	10
D <sub>2</sub> , 760	0.6	2.4 (H <sub>2</sub> O)		27	18	45	10	4
D <sub>2</sub> , 100	0.6	1.7 (H <sub>2</sub> O)		59	traces <sup>d</sup>	41	traces	10
D <sub>2</sub> , 100	0.7	2.9 (H <sub>2</sub> O)		47	traces	53	traces	5
D <sub>2</sub> , 760	0.7	1.6 (MeOH)	3	64	9	18	9	4
D <sub>2</sub> , 760	0.6	2.4 (MeOH)	3	61	13	13	13	3
D <sub>2</sub> , 760	0.6	1.4 (MeOH)		70	5	20	5	25
D <sub>2</sub> , 760	0.5	2.4 (MeOH)		74	2	18	6	20
D <sub>2</sub> , 100	0.5	1.4 (MeOH)		71	traces	29	traces	29
D <sub>2</sub> , 100	0.6	2.6 (MeOH)		70	traces	30	traces	18
CH <sub>4</sub> , 760	0.7	2.2 (H <sub>2</sub> O)	3	50	50	traces	nd <sup>e</sup>	1
CH <sub>4</sub> , 760	0.5	1.8 (H <sub>2</sub> O)		67	33	traces	nd	3
CH <sub>4</sub> , 100	0.4	1.3 (H <sub>2</sub> O)		100	traces	traces	nd	16
CH <sub>4</sub> , 760	0.7	1.9 (MeOH)	3	67	33	traces	nd	2
CH <sub>4</sub> , 760	0.7	1.6 (MeOH)		91	9	traces	nd	8
CH <sub>4</sub> , 100	0.7	1.9 (MeOH)		100	traces	traces	nd	18
C <sub>3</sub> H <sub>8</sub> , 760	0.7	2.0 (H <sub>2</sub> O)	3	traces	traces	traces	nd	
C <sub>3</sub> H <sub>8</sub> , 760	0.7	2.1 (H <sub>2</sub> O)		14	86	traces	nd	5
C <sub>3</sub> H <sub>8</sub> , 100	0.8	2.5 (H <sub>2</sub> O)		78	22	traces	nd	8
C <sub>3</sub> H <sub>8</sub> , 760	0.6	1.8 (MeOH)	3	traces	traces	traces	nd	
C <sub>3</sub> H <sub>8</sub> , 760	0.8	2.2 (MeOH)		27	73	traces	nd	4
C <sub>3</sub> H <sub>8</sub> , 100	0.7	2.0 (MeOH)		87	23	traces	nd	9

<sup>a</sup> A thermal radical scavenger, O<sub>2</sub> (4 Torr), is present in each experiment. Radiation dose:  $1.5 \times 10^4$  Gy (dose rate:  $10^4$  Gy h<sup>-1</sup>). <sup>b</sup> Ratio of the yield of each product to the combined yield of all products identified. The yields of the other conceivable isomeric products are below the detection limit of ca. 0.2%. Each value is the average of several determinations, with an uncertainty level of ca. 5%. <sup>c</sup> Absolute yields estimated from the percent ratio between the combined  $G(\text{products})$  value of the recovered products and the literature  $G(D_3^+) = 3$  (ref 12);  $G(C_nH_5^+) = 1.9$  ( $n = 1$ ),  $0.9$  ( $n = 2$ ) (ref 13); and  $G(i-C_3H_7^+) = 3$  (ref 18). The  $G(M)$  values are defined as the number of species produced per 100 eV of absorbed energy. <sup>d</sup> Traces = <0.5%. <sup>e</sup> Below detection limit, ca. 0.2%.

systems (Table I), under largely different experimental conditions. The considerable complexity of the product pattern, in the decay experiments, is reduced significantly in the radiolytic runs. Thus, only four products, *i.e.* 11–14, are recovered from the  $D_3^+$  experiments (Table II). Compounds 15 and 16, relatively abundant in the decay mixtures (Table I), could not be detected. The product pattern becomes even simpler in the  $C_nH_5^+$  and  $i-C_3H_7^+$  experiments, where only two products, *i.e.* 11 and 12, are recovered in appreciable yields.

The relative product distribution (Table II), while only slightly influenced by the presence of NMe<sub>3</sub>, depends on the total pressure of the system and the nature and the concentration of the nucleophile NuH. In general, a pronounced decrease of the relative yield of 12, mostly counterbalanced by a parallel increase of the relative yield of 11, is observed by decreasing the total pressure of the system. There is therefore a substantial insensitivity of the combined relative yields of 11 and 12 as a function of the experimental conditions, as shown by the limited variation of the (11 + 12)/(13 + 14) yield ratio (0.8–1.4 (NuH = H<sub>2</sub>O); 2.3–3.2 (NuH = MeOH)) by a more than 7-fold variation of the total pressure in the  $D_3^+$  systems.

**Fourier-Transform Ion-Cyclotron Resonance (FT-ICR) Mass Spectrometry.** FT-ICR measurements of the equilibrium constants for the proton-transfer reaction between 10 and reference bases, such as CH<sub>3</sub>CN and CH<sub>3</sub>COOH, allowed accurate determination of the gas-phase basicity of 10,  $182.2 \pm 1$  kcal mol<sup>-1</sup>. Taking into account the usual assumptions for the proton-transfer entropy contribution,  $7.75$  kcal mol<sup>-1</sup>, the proton affinity (PA) of 10 can be estimated as  $190 \pm 1$  kcal mol<sup>-1</sup>. From the

(20) There are considerable uncertainties as to the radiation dose actually absorbed by the gas and to the pressure dependence of the known  $G(D_3^+)$ ,  $G(C_nH_5^+)$ , and  $G(i-C_3H_7^+)$  values. In addition, there are several reaction channels available to the gaseous Brønsted acids following their attack on spiropentane that represents only one of the nucleophiles present in the irradiated systems.

**Table III.** Reaction Enthalpies<sup>a</sup>

$AH^+ + \text{Spiropentane} \rightarrow C_5H_6^+ + A + \Delta H^\circ$ 10			
gaseous Brønsted acid (AH <sup>+</sup> )	$-\Delta H^\circ$ (kcal mol <sup>-1</sup> )	gaseous Brønsted acid (AH <sup>+</sup> )	$-\Delta H^\circ$ (kcal mol <sup>-1</sup> )
<sup>3</sup> HeT <sup>+</sup>	144	C <sub>2</sub> H <sub>5</sub> <sup>+</sup>	28
D <sub>3</sub> <sup>+</sup>	89	<i>i</i> -C <sub>3</sub> H <sub>7</sub> <sup>+</sup>	10
CH <sub>3</sub> <sup>+</sup>	58		

<sup>a</sup> The formation enthalpies of the ions and the neutrals used for these calculations have been taken from ref 21. The heats of formation of <sup>3</sup>HeT<sup>+</sup> and D<sub>3</sub><sup>+</sup> are taken to be equal to those of <sup>4</sup>HeH<sup>+</sup> and H<sub>3</sub><sup>+</sup>, respectively. The heats of formation of C<sub>5</sub>H<sub>8</sub>T<sup>+</sup> and C<sub>5</sub>H<sub>8</sub>D<sup>+</sup> ions from <sup>3</sup>HeT<sup>+</sup> and D<sub>3</sub><sup>+</sup> attack on 1 are taken to be equal to that of C<sub>5</sub>H<sub>5</sub><sup>+</sup>, *i.e.* 220 kcal mol<sup>-1</sup>, as calculated from equilibrium measurements.

formation enthalpy of the neutral spiropentane,  $44.2 \pm 0.2$  kcal mol<sup>-1</sup>,<sup>21</sup> the heat of formation of the initial, stable protonated spiropentane is  $220 \pm 1$  kcal mol<sup>-1</sup>. By using this value, the standard enthalpy changes of the gas-phase protonation of 10 by the selected Brønsted acids can be estimated as reported in Table III.

## Discussion

**Reagents.** The <sup>3</sup>HeT<sup>+</sup> ion generated in the ground state in ca. 95% yield from spontaneous β-decay of T<sub>2</sub><sup>16</sup> is responsible for the formation of the tritiated products of Table I.

The <sup>3</sup>HeT<sup>+</sup> ion is an exceedingly powerful Brønsted acid ( $H_f^\circ = 320$  kcal mol<sup>-1</sup>),<sup>22</sup> which is able to tritonate virtually all organic

(21) Lias, S. G.; Bartmess, J. E.; Liebman, J. F.; Holmes, J. L.; Levin, R. D.; Mallard, W. G. *J. Phys. Chem. Ref. Data* 1988, 17, Suppl. 1.

(22) Chupka, W. A.; Russel, M. E. *J. Chem. Phys.* 1968, 49, 5426.

molecules,<sup>23</sup> including cyclic<sup>24</sup> and bicyclic alkanes.<sup>25</sup> Considering the exceedingly high exothermicity of the  $^3\text{HeT}^+$  protonation, an indirect route to the tritonated cyclic substrate involves initial formation of open-chain tritonated intermediates which eventually lose a hydron to another substrate molecule *via* a much less exothermic process. In this way, open-chain isomers are extensively produced as well, especially from highly strained systems. The tritiated product pattern shown in Table I is typical.

The radiolytic experimental conditions, in particular the low concentration of spiropentane (**10**) (below *ca.* 0.7 mol %) in a large excess of the bulk gas ( $\text{D}_2$ ,  $\text{CH}_4$ , or  $\text{C}_3\text{H}_8$ ), ensure that direct radiolysis of the starting substrate does not compete significantly. The ionic nature of the radiolytic products (as well as of the labeled decay products of Table I) is ensured by the presence of an effective thermal radical scavenger ( $\text{O}_2$ : 4 Torr), present in the mixture at adequate concentrations (0.5–3.7 mol %), and confirmed by the dramatic decrease (50–90%) of the overall product yields caused by addition to the gaseous mixture of 0.4 mol % (40 % in the decay runs) of  $\text{NMe}_3$ , an efficient Brønsted acid interceptor.

The major ionic species arising from the  $\gamma$ -radiolysis of  $\text{D}_2$ ,  $\text{CH}_4$ , and  $\text{C}_3\text{H}_8$  are  $\text{D}_3^+$ ,<sup>17</sup>  $\text{C}_n\text{H}_5^+$  ( $n = 1, 2$ ),<sup>18</sup> and  $i\text{-C}_3\text{H}_7^+$ , respectively.<sup>19</sup> That these ions function as gaseous Brønsted acids toward hydrocarbons has been established by independent mass spectrometric<sup>26</sup> and radiolytic studies.<sup>27</sup> Such ionic Brønsted acids, thermalized by many unreactive collisions with their parent molecules, eventually attack spiropentane (**10**), present in low concentrations (<0.7 mol %) in the gaseous mixture. The  $\text{C}_5\text{H}_9^+$  ions are formed with excess energy, which depends on the exothermicity of the process involved (Table III). In competition with quenching by unreactive collisions with the bulk gas molecules, the excited  $\text{C}_5\text{H}_9^+$  ions may undergo fragmentation and/or isomerization to more stable structures prior to neutralization by collision with a suitable acceptor, *e.g.* the added nucleophiles.

**Trapping Reactions.** The population of the isomeric  $\text{C}_5\text{H}_9^+$  ions from protonation of spiropentane (**10**) was sampled by introducing a known amount of a nucleophile, such as  $\text{H}_2\text{O}$  or  $\text{MeOH}$ , into the gaseous mixtures. Such nucleophiles react efficiently with the carbocations to yield O-protonated derivatives ( $\text{C}_5\text{H}_9\text{OHR}^+$ ;  $\text{R} = \text{H}$  or  $\text{Me}$ ). These products, in turn, eventually lose a proton to a suitable base, either deliberately added to the gaseous mixture (*e.g.*  $\text{NMe}_3$ ) or formed from radiolysis (*e.g.*  $\text{CH}_2\text{O}$ , etc.). Use of nucleophiles, NuH, such as  $\text{H}_2\text{O}$  ( $\text{PA} = 166.5 \text{ kcal mol}^{-1}$ )<sup>21</sup> and  $\text{MeOH}$  ( $\text{PA} = 181.9 \text{ kcal mol}^{-1}$ ),<sup>21</sup> precludes the occurrence of alternative pathways, such as proton loss from  $\text{C}_5\text{H}_9^+$  to NuH to yield the corresponding  $\text{C}_5\text{H}_8$  olefins ( $\text{PA} > 183 \text{ kcal mol}^{-1}$ ).<sup>21</sup> Their formation would complicate the neutral product pattern and thus the accurate determination of the  $\text{C}_5\text{H}_9^+$  isomeric distribution.

Both  $\text{H}_2\text{O}$  and  $\text{MeOH}$  are able to trap not only the  $\text{C}_5\text{H}_9^+$  ions but also their parent Brønsted acid(s). The fate of the daughter oxonium ions, mainly  $\text{H}_3\text{O}^+$  or  $\text{MeOH}_2^+$ , is determined by the composition of the gaseous mixture. In the decay samples, where the concentration of spiropentane (**10**) normally exceeds that of NuH (Table I), the oxonium ion  $\text{NuHT}^+$  formed from  $^3\text{HeT}^+$  attack on NuH may lose a hydron to **10**, rather than undergo clustering by NuH molecules. Primary isotope effect suggests that proton transfer rather than triton transfer from  $\text{NuHT}^+$  to **10** should take place preferentially. As a consequence, in the

decay runs, NuH may act as a sink of tritium labels as well, thus reducing the total activity of the recovered labeled products to an extent increasing with the NuH molar fraction (Table I). In the radiolytic systems where the concentration of **10** is low relative to that of NuH (Table II), extensive  $\text{NuH}_2^+$  ion association to NuH molecules may instead take place,<sup>28</sup> yielding relatively large proton-bound clusters whose ability to transfer a proton to **10** is drastically reduced.<sup>29</sup> Accordingly, irrespective of the specific NuH nucleophile employed, a pronounced decrease in the overall product yield is observed by increasing the NuH concentration. However, it cannot be excluded that a certain fraction of  $\text{NuH}_2^+$  ions does escape multiple clustering and, hence, can still protonate **10**, thus contributing to the formation of the neutral products. In this case, the product distribution is altered by the contribution of initial  $\text{C}_5\text{H}_9^+$  ions, directly arising from the gaseous Brønsted acids, and higher-order  $\text{C}_5\text{H}_9^+$  ions, generated with a lower excitation energy from the much less exothermic proton transfer from  $\text{NuH}_2^+$  to **10**. Accordingly, at comparable NuH concentrations, a distinct dependence of the product distribution upon the nature of NuH is observed (Table II). Furthermore, as expected, an inverse correlation is invariably found (Table II) between the exothermicity of the higher-order  $\text{C}_5\text{H}_9^+$  formation reaction from  $\text{NuH}_2^+$  and the relative yield of the kinetically most favored  $\text{C}_5\text{H}_9^+$  isomeric structure, *i.e.* that producing **11** (*vide infra*). This argument excludes a conceivable, alternative explanation of the influence of NuH on the product distribution, namely, that attack of  $\text{C}_5\text{H}_9^+$  on NuH occurs to give  $\text{C}_5\text{H}_9\text{NuH}^+$ , and that this adduct rearranges to give the final products. This hypothesis would lead one to expect an increasingly facile isomerization to the thermodynamically most stable open-chain structures,<sup>30</sup> in contrast with experimental evidence (Table II).

Hence, the product patterns of Tables I and II should be representative of the corresponding  $\text{C}_5\text{H}_9^+$  isomeric distribution. However, it is possible that  $\text{NuH}_2^+$  is present among the gaseous Brønsted acids which give  $\text{C}_5\text{H}_9^+$  ions from **10**.

**Gas-Phase Protonation Process.** The pioneering *ab initio* calculations of Lehn and Wipff modeled (crudely by today's standards) proton approach to spiropentane (**10**) along the C(1)–C(2) bond (path a of Figure 1) and attack at the spiro C(3) carbon (path b) and at the center of the cyclopropane face (path c).<sup>31</sup> Proton approach toward the C(1)–C(3) bond (path d of Figure 1) was not considered.<sup>31</sup> The approximation did not allow structural relaxation.



Semiempirical computations,<sup>32</sup> later confirmed by mass spectrometric evidence,<sup>33</sup> indicate that **18** (path b of Figure 1) would twist and form the pyramidal intermediate **8** (Figure 2), which could open to the cyclopentyl cation (**1**) (Figure 2). Accordingly, species **18** may be the initial protonated spiropentane responsible for the formation of **1** *via* **8** and, hence, of its neutral derivative

(23) Cacace, F. *Adv. Phys. Org. Chem.* **1970**, *8*, 79.  
 (24) (a) Cacace, F.; Caroselli, M.; Cipollini, R.; Ciranni, G. *J. Am. Chem. Soc.* **1968**, *90*, 2222. (b) Cacace, F.; Guarino, A.; Possagno, E. *J. Am. Chem. Soc.* **1969**, *91*, 3131. (c) Cacace, F.; Guarino, A.; Speranza, M. *J. Am. Chem. Soc.* **1971**, *93*, 1088.  
 (25) Cacace, F.; Guarino, A.; Speranza, M. *J. Chem. Soc. Perkin Trans. 2* **1973**, 66.  
 (26) Field, F. H. In *Ion-Molecule Reactions*; Franklin, J. L., Ed.; Butterworths: London, 1972; Vol. 1.  
 (27) (a) Ausloos, P.; Lias, S. G. In *Ion-Molecule Reactions*; Franklin, J. L., Ed.; Butterworths: London, 1972; Vol. 2. (b) Lias, S. G. In *Interactions between Ions and Molecules*; Ausloos, P., Ed.; Plenum: New York, 1974.

(28) (a) Hermann, V.; Kay, B. D.; Castleman, A. W., Jr. *Chem. Phys.* **1982**, *72*, 185. (b) Lau, Y. K.; Ikuta, S.; Kebarle, P. *J. Am. Chem. Soc.* **1982**, *104*, 1462. (c) Meot-Ner, M.; Field, F. H. *J. Am. Chem. Soc.* **1977**, *99*, 998. (d) Cunningham, A. J.; Payzant, J. D.; Kebarle, P. *J. Am. Chem. Soc.* **1972**, *94*, 7627. (e) Beggs, D. P.; Field, F. H. *J. Am. Chem. Soc.* **1971**, *93*, 1567. (f) Kebarle, P.; Searles, S. K.; Zolla, A.; Scarborough, J.; Arshadi, M. *J. Am. Chem. Soc.* **1967**, *89*, 6393. (g) Grimsrud, E. P.; Kebarle, P. *J. Am. Chem. Soc.* **1973**, *95*, 7939.

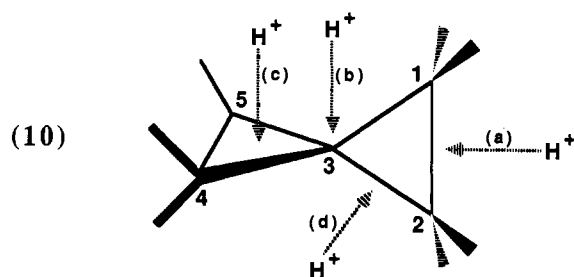
(29) (a) Bohme, D. K.; MacKay, G. I.; Tanner, S. D. *J. Am. Chem. Soc.* **1979**, *101*, 3724. (b) Morgan, S.; Castleman, A. W., Jr. *J. Am. Chem. Soc.* **1987**, *109*, 2867.  
 (30) For instance, closed-shell cyclopropylcarbenium and cyclopropyloxonium ions, if sufficiently activated, tend to isomerize to their more stable acyclic structures (see, for instance: Schwarz, H. In *The Chemistry of Cyclopropyl Groups*; Rappoport, Z., Ed.; Wiley: New York, 1987).

(31) Lehn, J. M.; Wipff, G. *J. Chem. Soc., Chem. Commun.* **1973**, 747.

**Table IV.** Computed HF and MP2(FULL) Absolute (au) and Relative Energies (kcal/mol) of  $C_5H_9^+$  Ions

species	theoretical level						
	HF/6-31G*			MP2/6-31G*			
	abs energy (au)	rel energy (kcal/mol)	NIMAG <sup>a</sup>	abs energy (au)	ZPE (kcal/mol)	rel energy <sup>b</sup> (kcal/mol)	NIMAG = 1 (cm <sup>-1</sup> )
1	-194.292 84	0.0	0	-194.938 24	84.9	0.0	
2	-194.277 02	9.9	0	-194.936 74	84.8	0.8	
2'	-194.275 39	10.9	1	-194.934 30	83.7	1.3	-171
3	-194.284 55	5.2	0	-194.937 40	84.4	0.0	
4	-194.281 08	7.4	0	-194.934 61	84.6	2.0	
5	-194.302 26	-5.9	0	-194.943 23	83.5	-4.6	
6	-194.309 54	-10.5	0	-194.949 01	83.6	-8.1	
7	-194.290 53	1.5	0	-194.929 22	84.3	5.1	
8	-194.251 16	26.2	0	-194.917 85	85.5	13.4	
9	-194.241 89	32.0	1	-194.908 00	86.0	20.1	
17	-194.239 46	33.5	1	-194.889 96	83.1	28.5	-12
18	-194.221 27	43.7	1	-194.881 00	84.8	35.8	-180
19	-194.215 53	48.5	1	-194.879 51	83.5	35.5	
20	-194.271 57	13.3	0	-194.912 26	84.2	15.6	
21	-194.267 58	15.9	1	-194.925 55	84.1	7.2	-75
21'	-194.266 58	16.5	1	-194.924 19	84.0	7.9	-138
22	-194.275 21	11.1	1	-194.919 01	82.9	10.1	

<sup>a</sup> Number of imaginary frequencies. <sup>b</sup> Including ZPE contribution.



**Figure 1.** Conceivable pathways for the approach of a proton toward spirocyclopentane.

14 in the decay ( $^3\text{HeT}^+$ ; Table I) and radiolytic experiments ( $\text{D}_3^+$ ; Table II). All the other neutral products of Tables I and II probably originate from the primary species 17 (path d of Figure 1).

Evidence in favor of a relatively stable intermediate 17 is provided by the isolation of appreciable amounts of tritiated spirocyclopentane 10' from the decay experiments (Table I).  $C_5H_9^+$  isomers (including 8) other than 17 cannot give back tritiated 10 by proton transfer to NuH, but rather add to it, yielding the neutral products 11–16. Formation of 10' can only be explained by the existence of structure 17, in which the closed spirobicyclic geometry is essentially retained.<sup>31</sup> Species 17 is long-lived enough to undergo a hydron loss to a suitable acceptor, including another molecule of 10.<sup>34</sup> In this respect, assuming that hydron transfer from 17 to 10 takes place at the Langevin-calculated collision limit ( $k_L = 1.2 \times 10^{-9} \text{ cm}^3 \text{ molecule}^{-1} \text{ s}^{-1}$ ),<sup>35</sup> a lifetime in excess of  $7 \times 10^{-9} \text{ s}$  can be estimated for 17. This implies that, in the gas phase, 17, is a relatively long-lived intermediate, separated from the open-chain isomers by a significant activation barrier. Hence, bond cleavage in 17 should be slow relative to proton transfer to 10, under the experimental conditions.

Independent support in favor of relatively stable structures 17 and 8 is provided by *ab initio* calculations. MP2/6-31G\* is recognized as the minimum level of theory capable of furnishing a reasonably accurate description of carbocation potential energy

(32) Franke, W.; Schwarz, H.; Thies, H.; Chandrasekhar, J.; Schleyer, P. v. R.; Hehre, W. J.; Saunders, M.; Walker, G. *Angew. Chem., Int. Ed. Engl.* **1980**, *19*, 485.

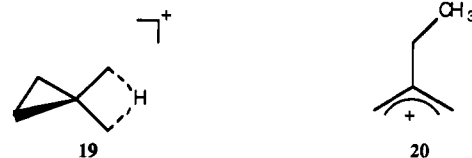
(33) Zummack, W.; Schwarz, H.; van Driel, J. H.; Terlouw, J. K. *Int. J. Mass Spectrom. Ion Processes* **1984**, *62*, 233.

(34) According to the heat of formation of 17 ( $H_f^\circ = 220 \pm 1 \text{ kcal mol}^{-1}$ ) calculated from FT-ICR proton-affinity equilibria measurements, neutralization of 17 by proton loss to  $\text{H}_2\text{O}$  and to MeOH is endothermic by 24 and 8 kcal mol<sup>-1</sup>, respectively (ref 21).

(35) Su, T.; Bowers, M. T. In *Gas-Phase Ion Chemistry*; Bowers, M. T., Ed.; Academic Press: New York, 1979.

surfaces.<sup>2,3b,i</sup> Seventeen  $C_5H_9^+$  stationary points were located first at HF/6-31G\*. These were characterized by vibrational frequency analysis. All these geometries were reoptimized at MP2(FULL)/6-31G\*, and, for some, post-HF vibrational frequencies were computed analytically. The protonated spirocyclopentane 17 was further investigated at MP2(FC)/6-31G\*\* to correct the artificial imaginary frequency which wrongly characterizes 17 as a transition state at MP2(FULL)/6-31G\*. Figures 2 and 3 depict the MP2(FULL)/6-31G\* geometries; the energies are given in Table IV. The relative energies are based on the  $C_2$ -symmetric cyclopentyl cation (1).<sup>6</sup>

When a proton is positioned at the center of the C(1)–C(2) bond (path a of Figure 1) and  $C_{2v}$  symmetry imposed, optimization gives the *edge*-protonated ion 19, which is less stable than 1 by 35.5 kcal mol<sup>-1</sup>. Ion 19 is a transition structure for the hydrogen shift to the equivalent C(1)H<sub>2</sub> or C(2)H<sub>2</sub> methylene groups. When the  $C_{2v}$  symmetry constraint was removed, thus allowing H movement toward C(1), the  $C_s$ -symmetric ethylallyl cation 20 was obtained. This is a minimum on the potential energy surface. Both cyclopropyl rings of 10 have opened fully. This open-chain structure is less stable than ion 1 by *ca.* 16 kcal mol<sup>-1</sup> (Table IV).



Proton approach along path b of Figure 1, *i.e.* toward the spiro carbon C(3), leads to ion 8 *via* the transition structure (TS) 18. The energy relative to 1 and 8 is 35.8 and 22.4 kcal mol<sup>-1</sup>, respectively. The imaginary frequency corresponds to a rotation of the C(1)H<sub>2</sub>–C(2)H<sub>2</sub> unit by 90°. The transition structure 9 connecting 8 with the cyclopentyl cation lies 6.7 kcal mol<sup>-1</sup> above 8.

Proton approach along path d (Figure 1) leads to 17 ( $C_s$  symmetry). This structure can be viewed as a corner-protonated spirocyclopentane, which retains the carbon skeleton of spirocyclopentane. Frequency analysis at MP2(FULL)/6-31G\* characterizes 17 as a transition state with the very small imaginary frequency of  $-12i \text{ cm}^{-1}$ . The reliability of this calculation must be doubted, so 17 was reoptimized at MP2(FC)/6-31G\*\*, and the frequency calculation at this level characterizes 17 as a minimum with the lowest frequency of  $+80 \text{ cm}^{-1}$ . This finding provides further support for the existence of a stable, corner-protonated spirocyclopentane intermediate. From Table IV, ion 17 is less stable than

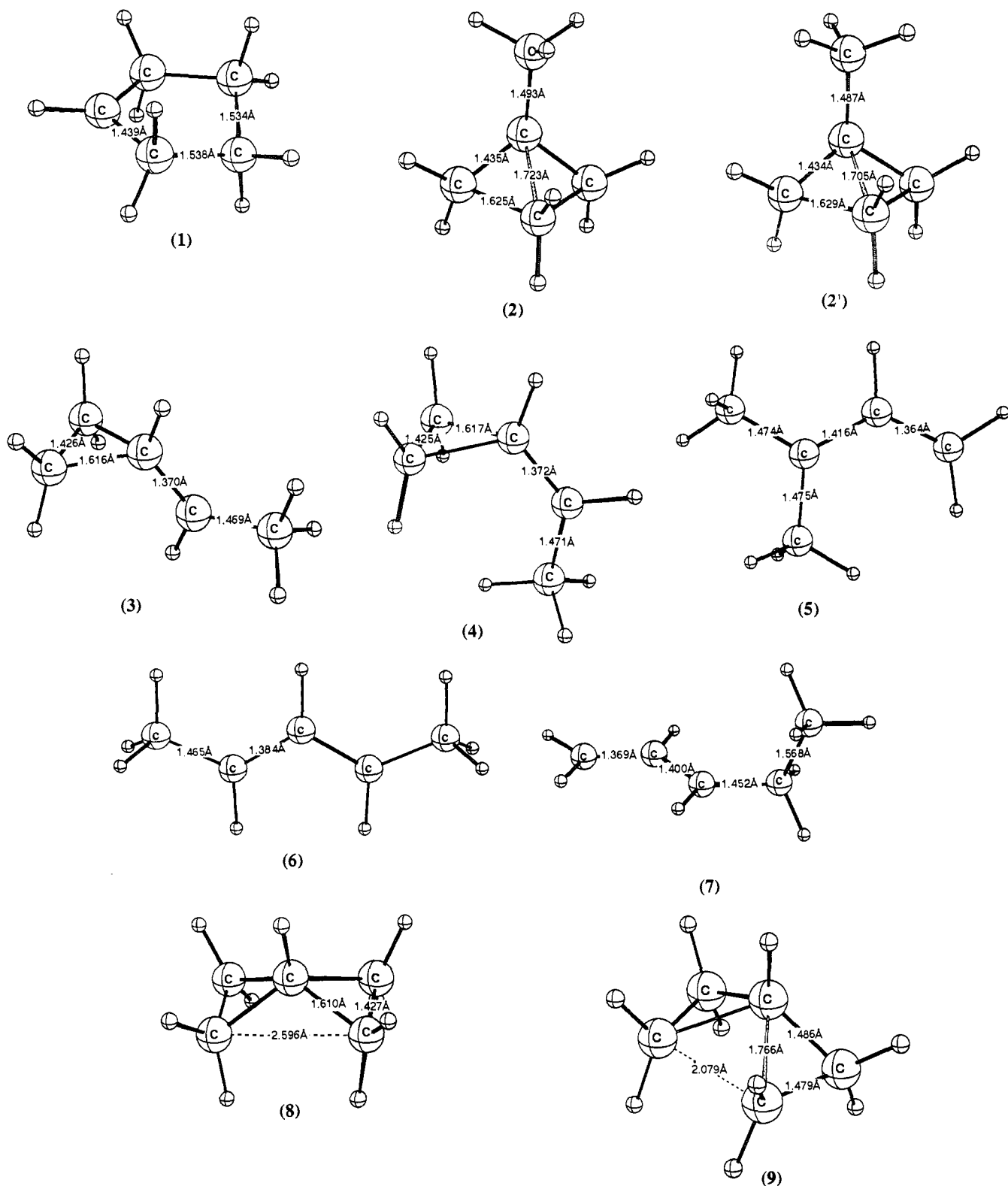
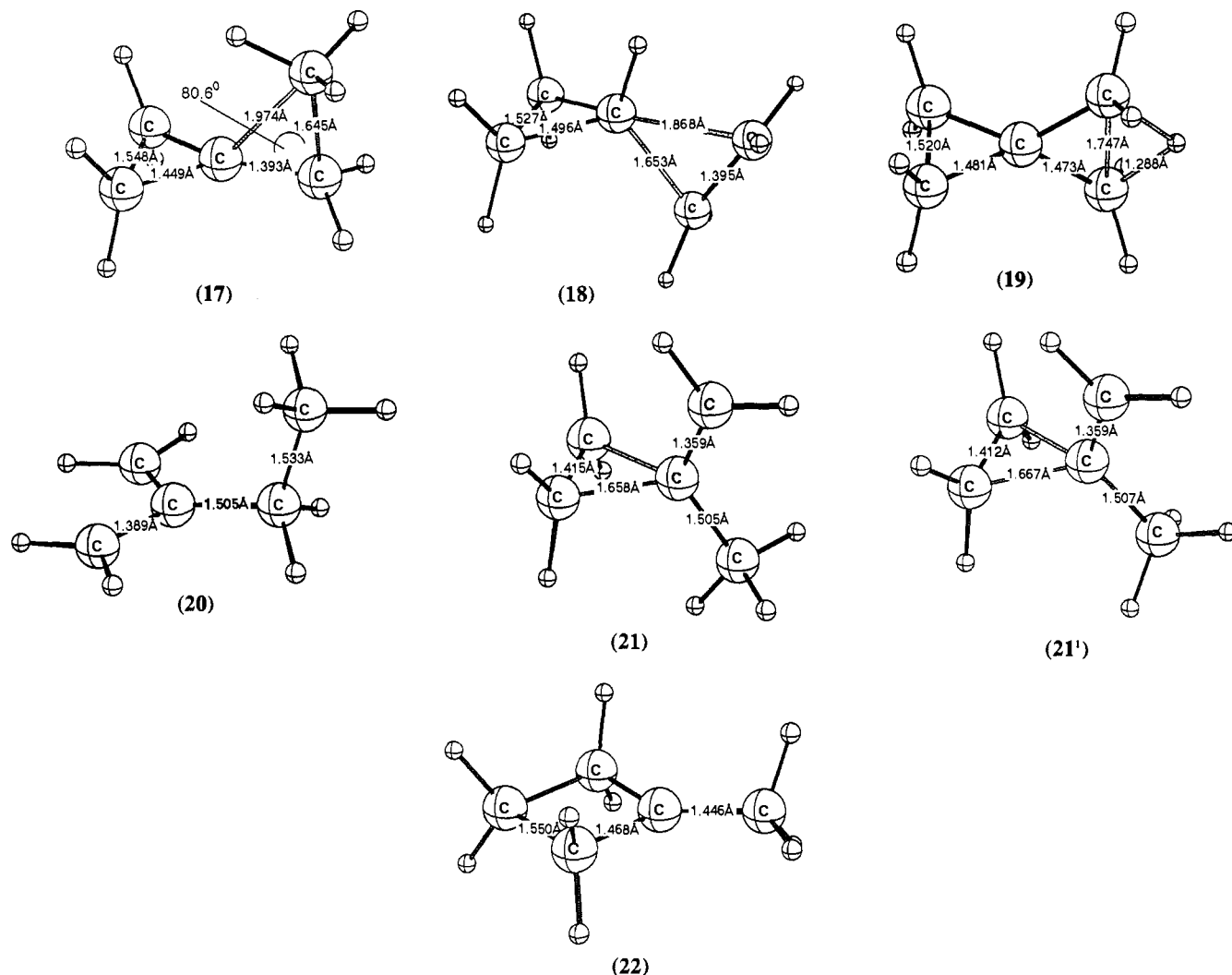


Figure 2. MP2/6-31G\*-optimized geometries of the investigated  $C_5H_9^+$  ions 1, 2, 2', and 3-9. Bond lengths are in angstroms and bond angles in degrees.

the cyclopentyl cation by 28.5 kcal mol<sup>-1</sup>. Since the experimental heat of formation of the latter species is 191 kcal mol<sup>-1</sup>,<sup>21</sup> we estimate the heat of formation of ion 18 to be 219.5 kcal mol<sup>-1</sup>. This value agrees remarkably well with the heat of formation of the structurally unknown  $C_5H_9^+$  ion, as obtained from the above described FT-ICR experiments, 220 ± 1 kcal mol<sup>-1</sup>, thus suggesting the formation of this species as the stable intermediate from almost thermoneutral gas-phase protonation of spiropentane.

We next tackled the question of the existence of the *bisected* (1-methylcyclopropyl)carbanyl and the 1-methylcyclobutyl cations,<sup>8</sup> which are possible precursors to the final products 16 and

15, respectively. Two distinct conformations of the (1-methylcyclopropyl)carbanyl cation have been located on the MP2-(FULL)/6-31G\* potential energy surface, *i.e.* ions 21 and 21'. These two species are within 1 kcal mol<sup>-1</sup> in energy and differ only in the conformation of the CH<sub>3</sub> group. The more stable of the two, 21, is *ca.* 7 kcal mol<sup>-1</sup> above 1 in energy. From the examination of the MP2/6-31G\* vibrational frequencies, none of these species actually corresponds to a minimum on the surface. Imaginary frequencies of -75i and -138i cm<sup>-1</sup> have been computed for 21 and 21', respectively. Even at MP2(FC)/6-31G\*\* 21 retains one imaginary frequency of -72i cm<sup>-1</sup>. From the



**Figure 3.** MP2/6-31G\*-optimized geometries of the investigated  $C_5H_9^+$  ions 17–21, 21', and 22. Bond lengths are in angstroms and bond angles in degrees.

examination of the corresponding vibrational modes, both of these species are unstable toward formation of the stable nonplanar 1-methylcyclobutyl ion **2**, which is more stable than ion **21** by 6.4 kcal mol<sup>-1</sup>. The planar 1-methylcyclobutyl cation **22** is not a minimum on the surface, and it is less stable than ion **2** by 9.3 kcal mol<sup>-1</sup>.



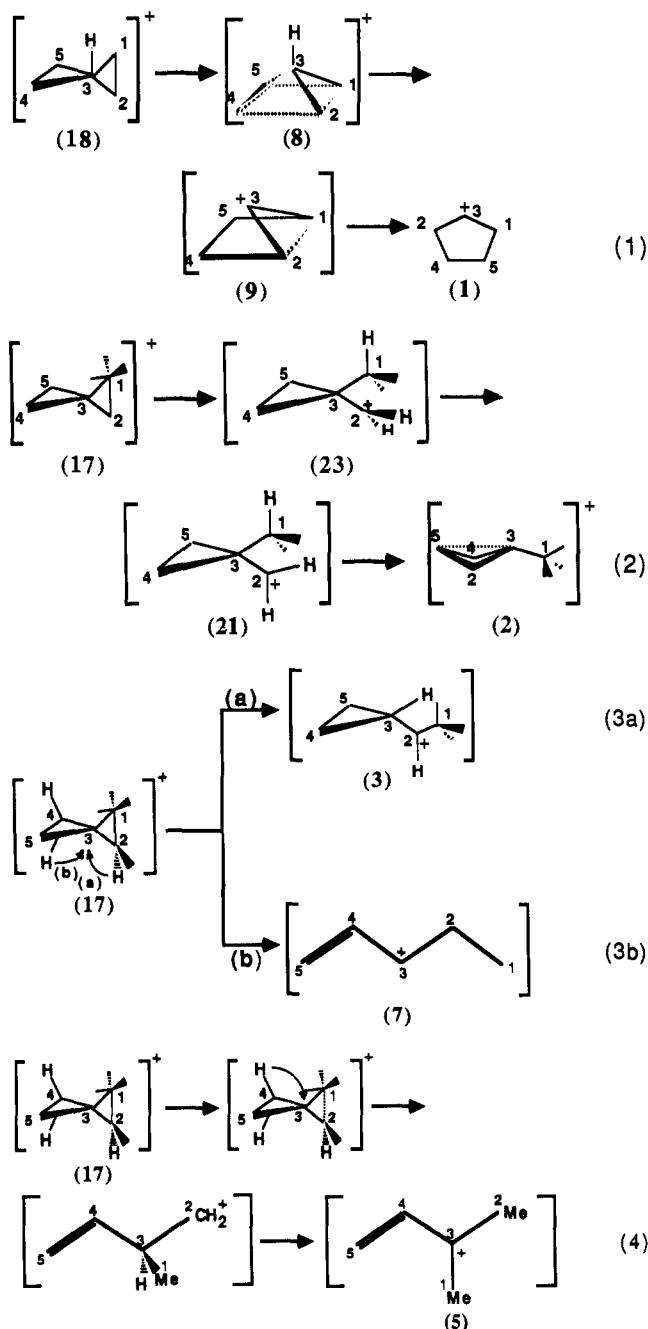
Finally the stable ion **4** was located on the  $C_5H_9^+$  potential energy surface. From Table IV, it is degenerate with the stable  $C_2$  cyclopentyl cation.

In order to gain information about the relative stability of some open-chain  $C_5H_9^+$  structures, whose formation has been evidenced by the nuclear-decay and radiolytic experiments, calculations have been performed on the 1,1-dimethylallyl (**5**), 1,3-dimethylallyl (**6**), and 1-ethylallyl (**7**) cations. Ion **6** is the most stable species found in our study, with a relative energy of -8.1 kcal mol<sup>-1</sup> with respect to the cyclopentyl cation. Ion **7** is about 10 kcal mol<sup>-1</sup> higher in energy than **5**.

**Gas-Phase  $C_5H_9^+$  Isomerization Pattern.** The structure and the stability of the primary intermediates **17** and **8** from gas-phase protonation of **10** having been defined, it is now possible to analyze their evolution to the isomeric structures which

eventually yield the neutral products **11–16**. Here we point out that, despite its relative stability, structure **20** (Figure 3) appears inaccessible to gas-phase protonation of **10** under all conditions, as demonstrated by the persistent failure to detect 2-methylenebutyl-Nu (Nu = OH or OMe) among the decay and radiolytic products (Tables I and II). This implies either that path a of Figure 1 is kinetically disfavored relative to the competing pathways b–d or, more likely, that the ensuing protonated transient **19** immediately rearranges to the more stable rotamer **17** prior to significant C(1)–C(3) bond fission. Thus, irrespective of its detailed dynamics (paths a–d of Figure 1), gas-phase protonation of **10** leads to the primary intermediates **17** and **8**, whose relative proportions and fate are strictly dependent on the nature of the Brønsted acid employed. Decreasing the strength of the gaseous acid (in the order  ${}^3\text{HeT}^+ > \text{D}_3^+ > \text{CH}_5^+ > \text{C}_2\text{H}_5^+ > i\text{-C}_3\text{H}_7^+$ ; Table III) increases the percentage amount of products **11** and **12** which are derived from intermediate **17**. The formation of **14** occurs only when the most powerful, unselective  ${}^3\text{HeT}^+$  (Table I) and  $\text{D}_3^+$  acids (Table II) are used. This is suggestive of the competing occurrence of both **17** and **8**, with the first kinetically favored over the latter. Their different ease of formation is attributed to the high-energy initial structure **18** from path b of Figure 1, whose formation necessarily precludes the occurrence of **8** (eq 1).

An additional factor influencing the pattern and rate of isomerization of **17** and **8** is the excitation energy imparted to them upon protonation of **10**. In fact, decreasing the internal energy of **17** by decreasing the exothermicity of its formation



process (in the order  ${}^3\text{HeT}^+ > \text{D}_3^+ > \text{CH}_3^+ > \text{C}_2\text{H}_5^+ > i\text{-C}_3\text{H}_7^+$ ; Table III) leads to an increase of the relative amounts of **11** and **12**. This can be interpreted by assuming that isomerization of **17** leading to **3**, **4**, and **7** (eq 3) may involve lower activation barriers than the alternative rearrangement of **17** to **5** (eq 4) and **2** (eq 2).

In this framework, relatively abundant formation of labeled **15** (20–25%) and **16** (18–22%) is observed only when **17** is formed from the very exothermic  ${}^3\text{HeT}^+$  attack on **10** (Table I) and, hence, possesses the largest amount of excitation energy (Table III). This indicates that the isomerization of **17** to **2** is the process involving the highest activation energy. This process presumably involves C(1)–C(2) bond fission in **17** to a *perpendicular* (1-methylcyclopropyl)carbinyl structure (**23**), prior to its collapse to the *bisected* rotamer **21** and finally to the stable nonplanar 1-methylcyclobutyl ion (**2**) (eq 2). We have already shown in the previous section that **21** is not a minimum. Likewise we were unable to locate a structure corresponding to **23**; optimization with a geometry similar to **23** led back to **17**. Thus, both **21** and **23** can be considered as the transition structure connecting **17** with **2**, which is the precursor of both **15** and **16**. When

energetically accessible, isomerization of excited **17** to **2** takes place in a time which is short relative to the collisional time with a NuH molecule (*ca.*  $10^{-9}$  s), as suggested by the constancy of the **15/16** yield ratio (1.0–1.3) measured under all experimental conditions, which therefore approximately represents the relative reactivity of NuH toward the C(2) and C(3) centers of **2**.

**Comparison with Condensed-Phase Studies.** The general picture of the  $\text{C}_5\text{H}_9^+$  potential energy surface based on the present study conforms in part to the familiar  $\text{C}_5\text{H}_9^+$  ion pattern observed in low-nucleophilic media (Scheme I).<sup>8</sup>

In superacids, the  $\text{C}_5\text{H}_9^+$  isomerization pattern is characterized by a dynamic equilibrium between equivalent delocalized 1-methylcyclobutonium ion structures (**2**) through the (methylcyclopropyl)carbinyl cation, the latter being a transition state. At temperatures above  $-25$  °C, conversion of **2** to the 1-cyclopropylethyl structures **3** and **4** takes place with an activation barrier estimated to be as large as *ca.* 20 kcal mol<sup>-1</sup>.<sup>8</sup> Both the *cis* (**4**) and the *trans* isomers (**3**) of the 1-cyclopropylethyl cation form an equilibrium mixture in which interconversion takes place *via* the *anti*-1-ethylallyl cation (**7**), with an activation barrier of 12.4 kcal mol<sup>-1</sup>.<sup>8</sup> The energy required for a direct C<sub>ring</sub>–CHMe bond rotation was estimated to be *ca.* 19 kcal mol<sup>-1</sup>.<sup>8</sup> Rotamers **3** and **4** are separated energetically by 1.5 kcal mol<sup>-1</sup>,<sup>8</sup> which is in agreement with the 2.0 kcal mol<sup>-1</sup> found by computation at MP2(FULL)/6-31G\*.

The qualitative agreement between the gas-phase  $\text{C}_5\text{H}_9^+$  ion pattern and that observed in low-nucleophilicity media extends to the failure to observe the 2-ethylallyl structure (**20**), inaccessible under all conditions. In addition, the failure to detect the occurrence of the cyclopentyl cation (**1**) among the  $\text{C}_5\text{H}_9^+$  intermediates of Scheme I confirms the gas-phase evidence that **1** originates from a high-energy path (*via* **8**), opened only in the isolated state by protonation of **10** by the powerful, unselective  ${}^3\text{HeT}^+$  and  $\text{D}_3^+$  acids.

## Conclusions

Gas-phase protonation of spiropentane generates two initial  $\text{C}_5\text{H}_9^+$  species, *i.e.* **17** and **8**, whose relative abundance depends on the nature of the gaseous Brønsted-acid catalyst employed.

The nature and the distribution of the neutral products from the gas-phase protonation of spiropentane provide some evidence for the existence of the corner-protonated spiropentane ion (**17**) as a fully legitimate ionic intermediate in the dilute gas state, with a lifetime in excess of  $7 \times 10^{-9}$  s. The experimental evidence is consistent with theoretical calculations. In fact, the existence of a protonated spiropentane as a local minimum on the  $\text{C}_5\text{H}_9^+$  potential energy surface could be verified at the MP2(FC)/6-31G\*\* level of theory, whereas the same species appears wrongly to be a first-order saddle point with a very small imaginary frequency at MP2(FULL)/6-31G\*. The performance of the HF/6-31G\* and MP2/6-31G\* theoretical approaches is adequate in providing the rest of the  $\text{C}_5\text{H}_9^+$  stable isomers. The same stability order was found, although appreciable differences emerge from the two calculation levels as to the energy and the structure of the same ionic species. Occurrence of **17** as a stable  $\text{C}_5\text{H}_9^+$  species is justified by an intense bonding interaction between its formally vacant p-orbital and the vicinal methyl moiety, which makes ring opening to the *ca.* 30 kcal mol<sup>-1</sup> more stable **3**, **4**, and **2** isomers a comparatively slow process. No evidence for **17** has been obtained from condensed-phase studies. This is presumably due to the preferential stabilization of ions, such as **2** and **4**, through solvation or ion-pairing effects. The same factors account for the failure to observe **17** as a stable intermediate in low-nucleophilicity solvent systems, where the activation barriers for its conversion to **2** and **4** may become vanishingly small. Thermodynamically favored intermediates such as **2** and **5** are formed when **17** has a high internal energy content, as is the case when the protonating agent is  ${}^3\text{HeT}^+$  or  $\text{D}_3^+$ . Kinetically preferred





electrons). The vibrational frequencies were computed for all stationary points, in order to characterize them as minima, transition states, or higher-order saddle points.

**Acknowledgment.** This work was supported in Rome by the Ministero della Ricerca Scientifica e Tecnologica (MURST), the Research National Council (CNR, Progetto Finalizzato,

“Chimica Fine II”) of Italy and in Erlangen by the Fonds der Chemischen Industrie, the Convex Computer Corporation, the HLRZ Jülich, and the LRZ München. We also thank Prof. F. Cacace for his interest in this work, Prof. W. Koch for providing MP2/6-31G\* calculations of several C<sub>5</sub>H<sub>9</sub><sup>+</sup> isomers, and Dr. A. Dorigo for reading the manuscript critically.